Supplementary Materials

Copper(II) Lysinate and Pseudoproline Assistance in the Convergent Synthesis of the GLP-1 Receptor Agonists Liraglutide and Semaglutide

Ivan Guryanov,[*,‡,ǁ] Andrea Orlandin,[‡] Ivan De Paola[‡], Angelo Viola,[‡] Barbara Biondi,[§] Denis Badocco,[§] Fernando Formaggio,[§] Antonio Ricci,[*,‡] and Walter Cabri[‡†]

[‡]*Fresenius Kabi iPSUM Srl, via San Leonardo 23, Villadose (RO), 45010 Italy*
[§]*ICB, Padova Unit, CNR, Department of Chemistry, University of Padova, Padova, via Marzolo 1, 35131 Italy*
[ǁ]*Institute of Chemistry, St. Petersburg State University, St. Petersburg, Peterhof, Universitetskij pr. 26, 198504 Russia*
[†]*Department of Chemistry "Giacomo Ciamician", Alma Mater Studiorum – University of Bologna, via Selmi 2, 40126 Bologna*

Table of Contents

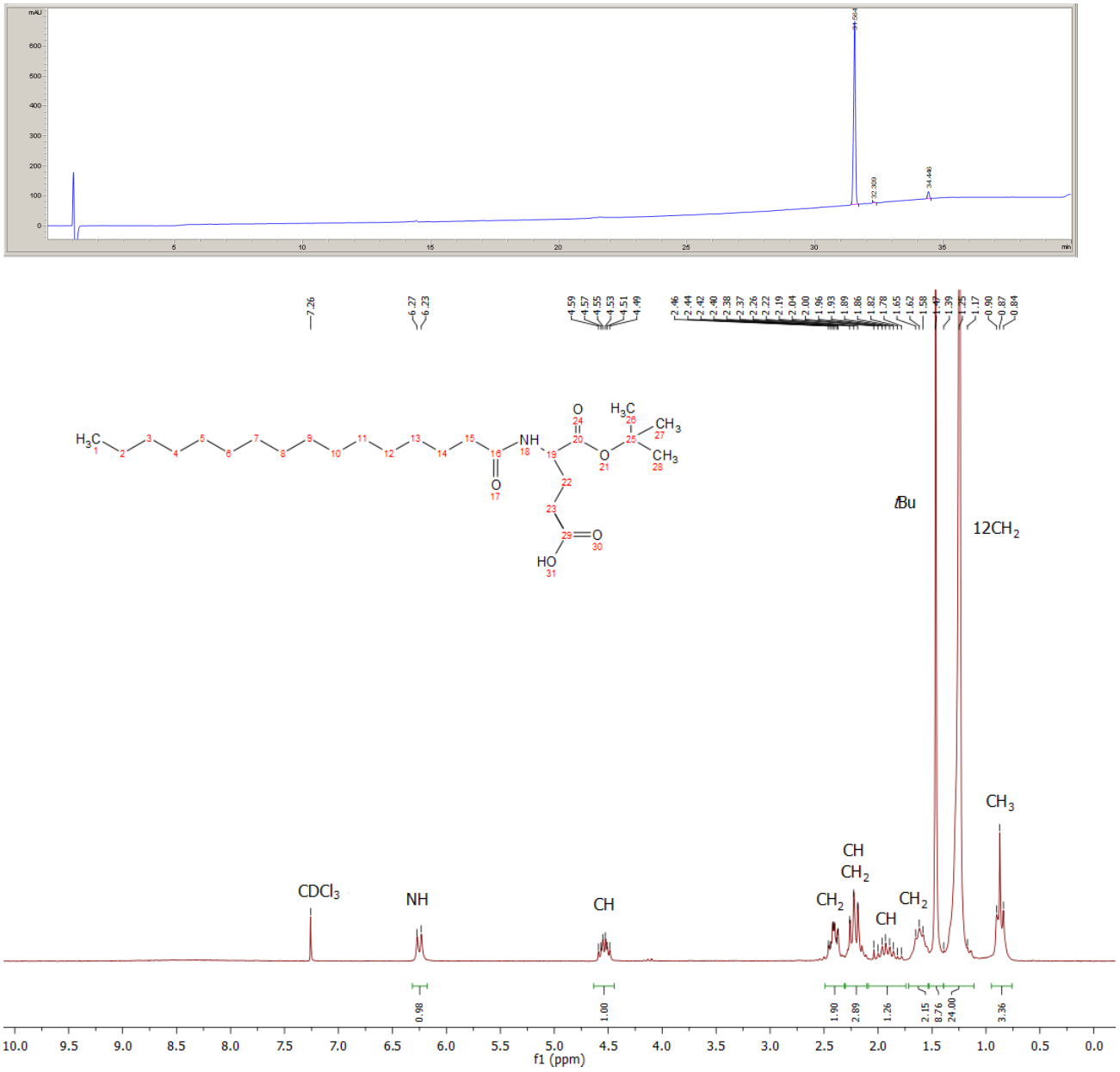

Figure S1. HPLC profile (top) and ^{1}H NMR spectrum (bottom) of Pal-Glu-O*t*Bu (Analytical method 1, see Experimental part).

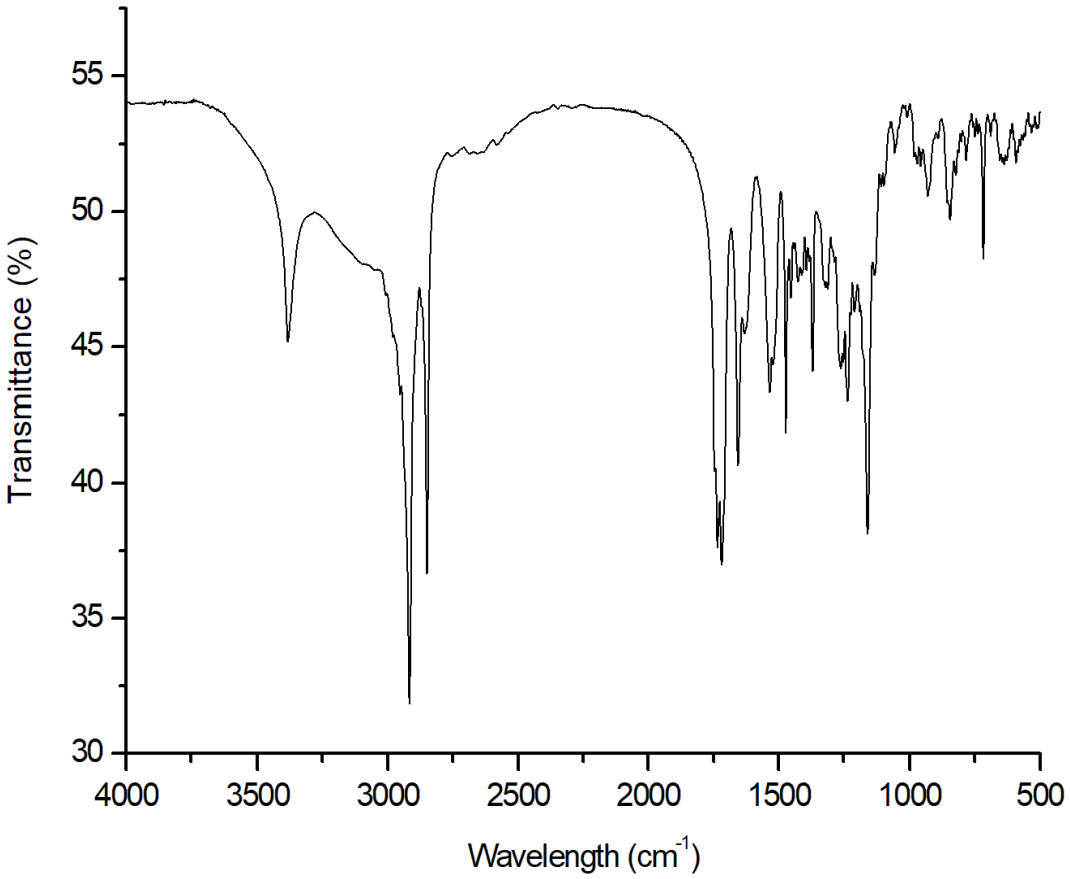

Figure S2. FT-IR spectrum of Pal-Glu-O*t*Bu (KBr).

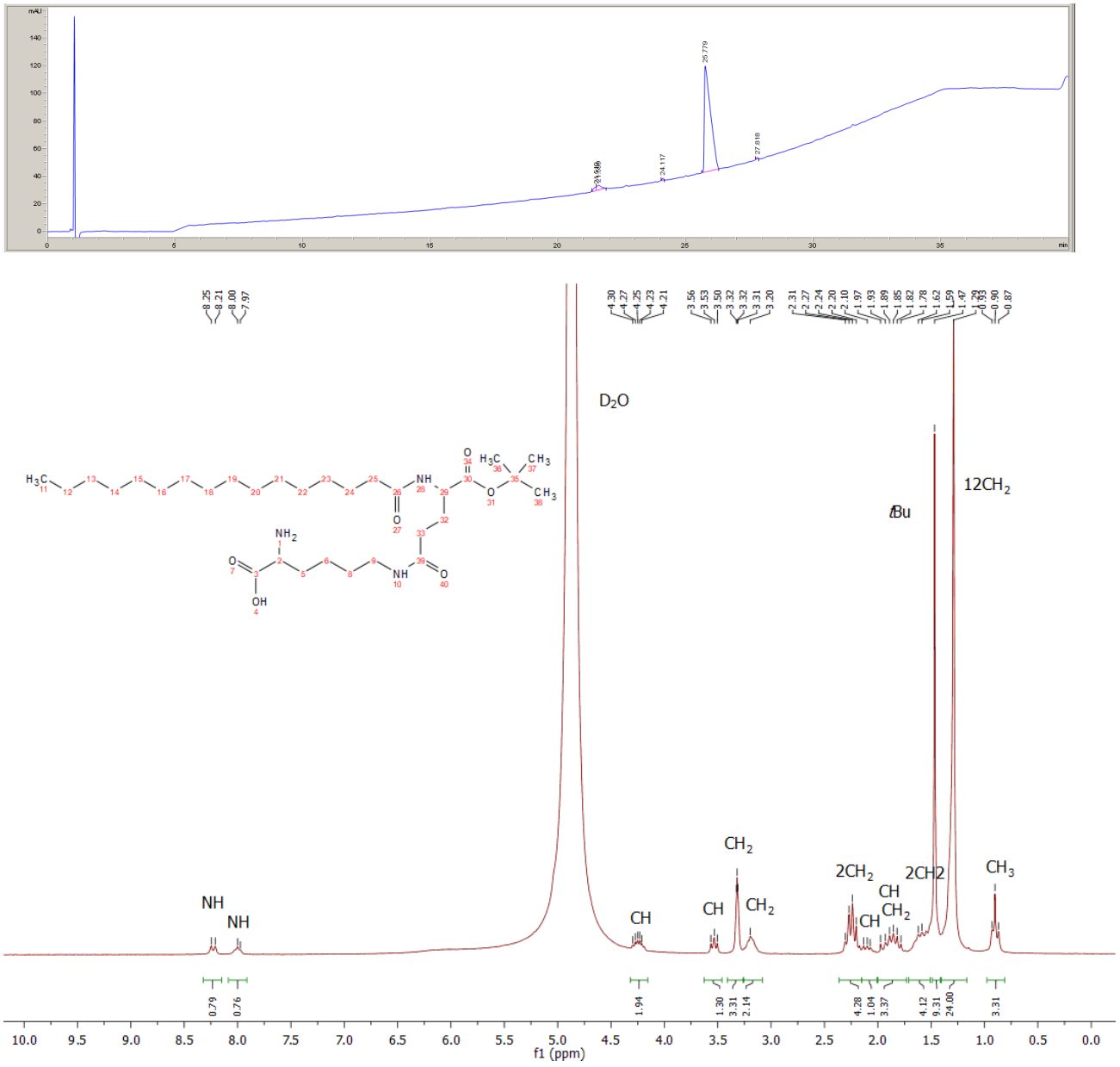

Figure S3. HPLC profile (top) and ^{1}H NMR spectrum (bottom) of H-Lys(Pal-Glu-O*t*Bu)-OH (Analytical method 1, see Experimental part).

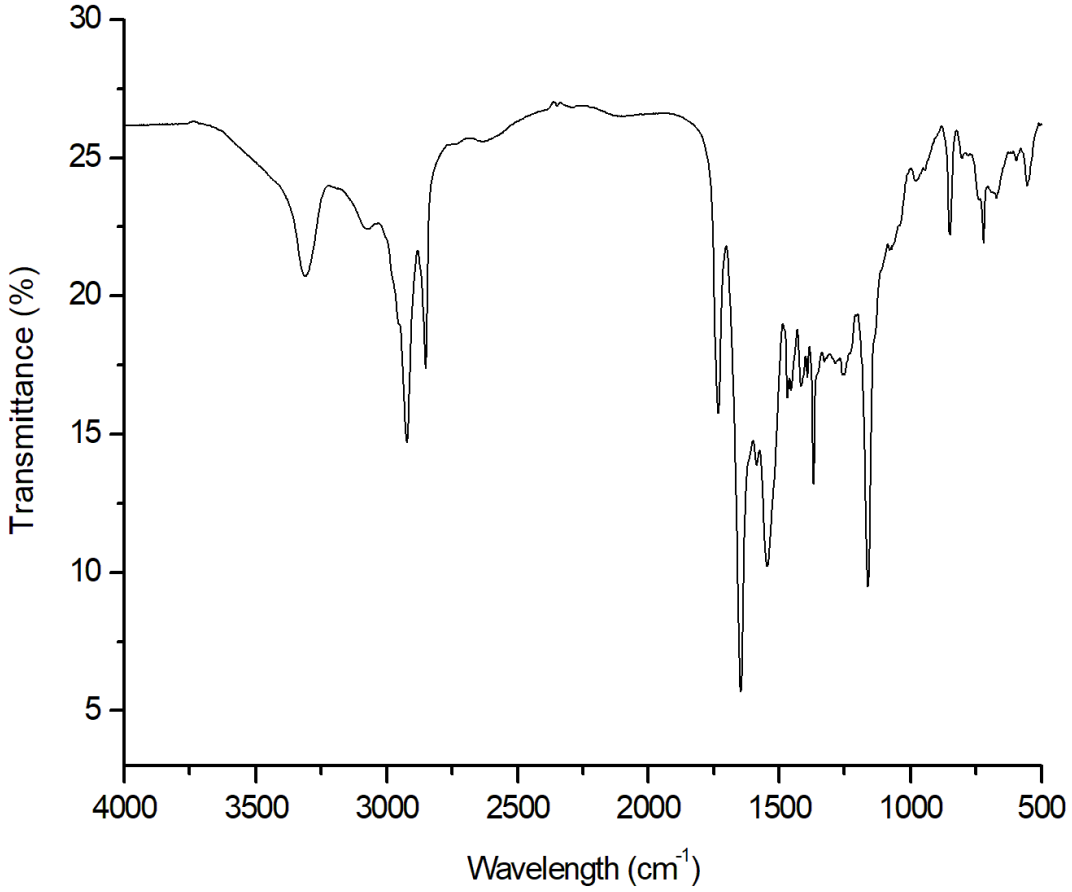

Figure S4. FT-IR spectrum of H-Lys(Pal-Glu-O*t*Bu)-OH (KBr).

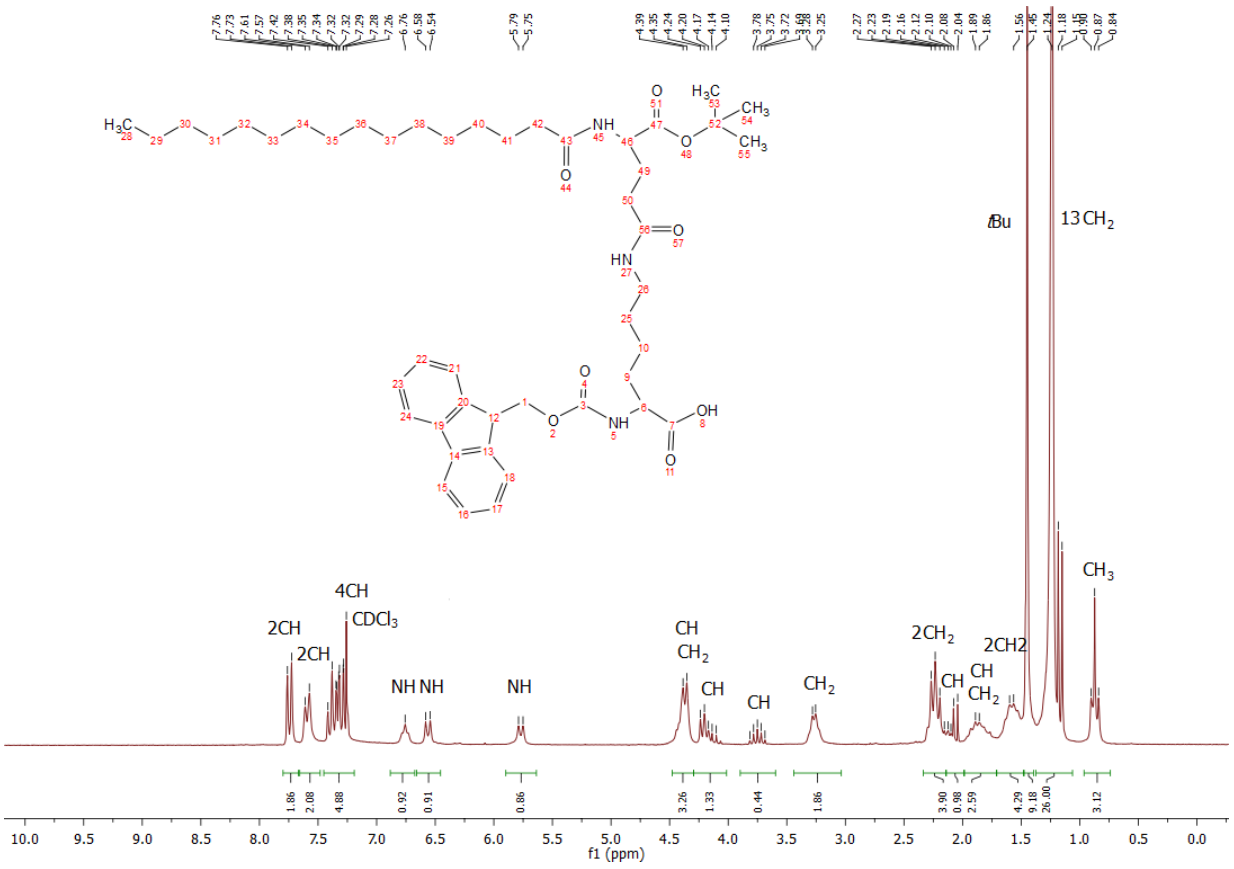

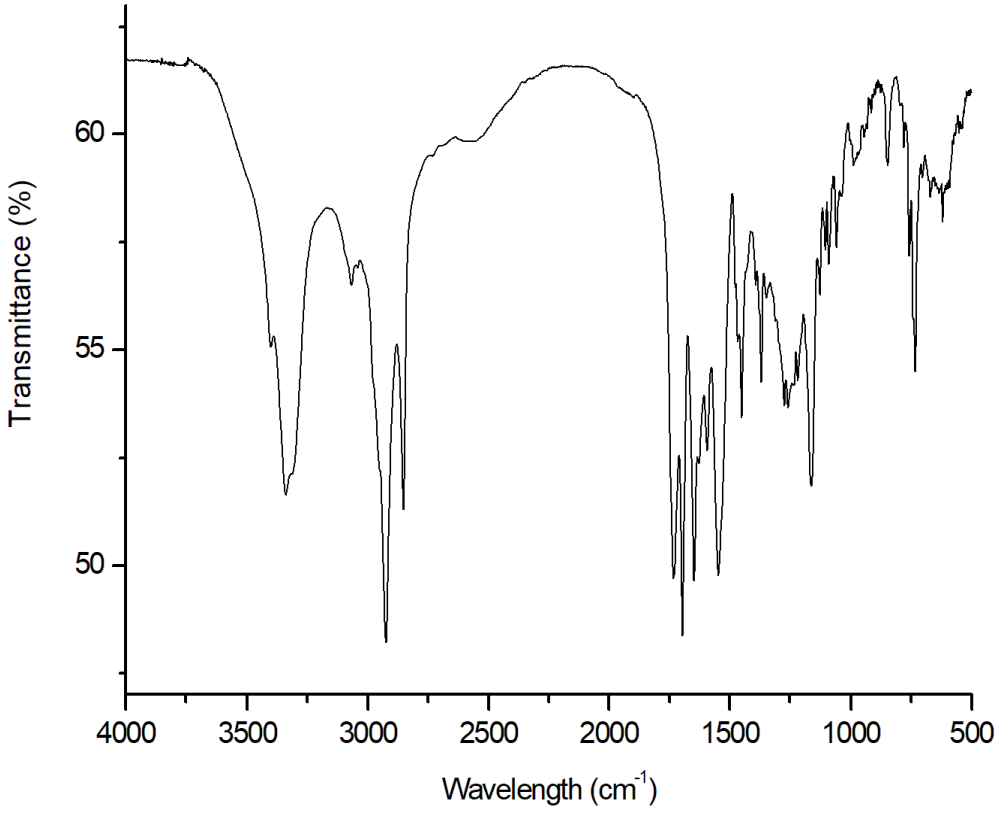

Figure S5. ^{1}H NMR (top) and FT-IR spectrum (bottom) of Fmoc-Lys(Pal-Glu-O*t*Bu)-OH.

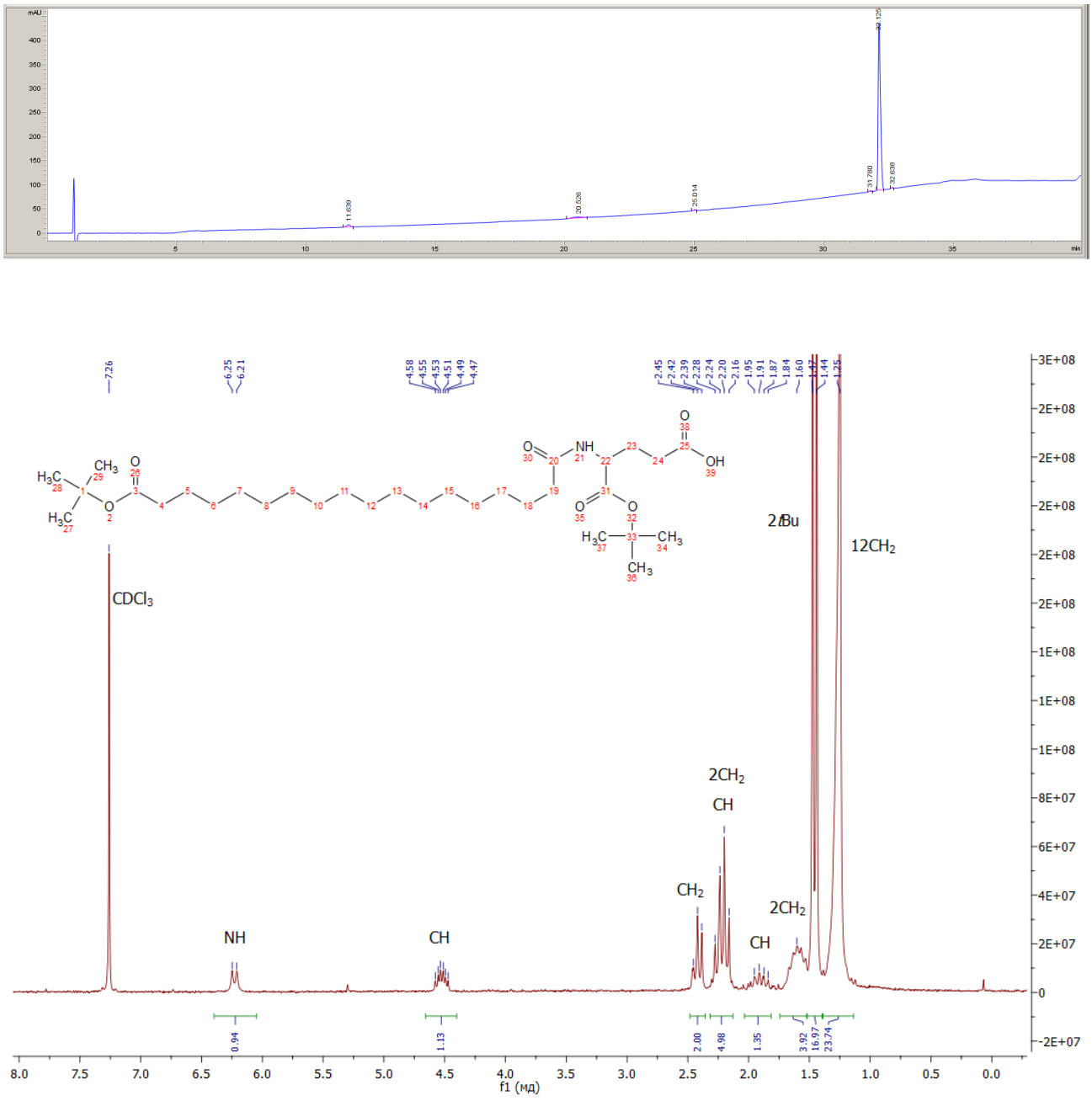

Figure S6. HPLC profile (top) and ^{1}H NMR spectrum (bottom) of *t*BuOCO-$(CH_2)_{16}$-CO-Glu-O*t*Bu (Analytical method 1, see Experimental part).

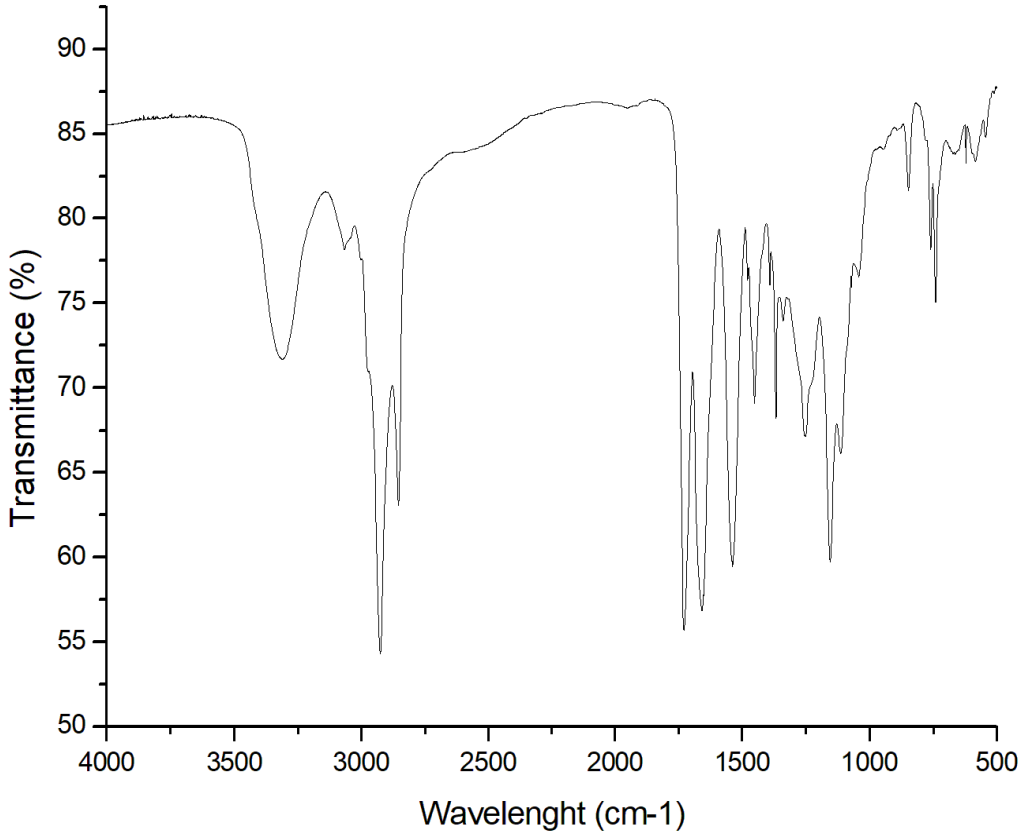

Figure S7. FT-IR spectrum of *t*BuOCO-$(CH_2)_{16}$-CO-Glu-O*t*Bu (KBr).

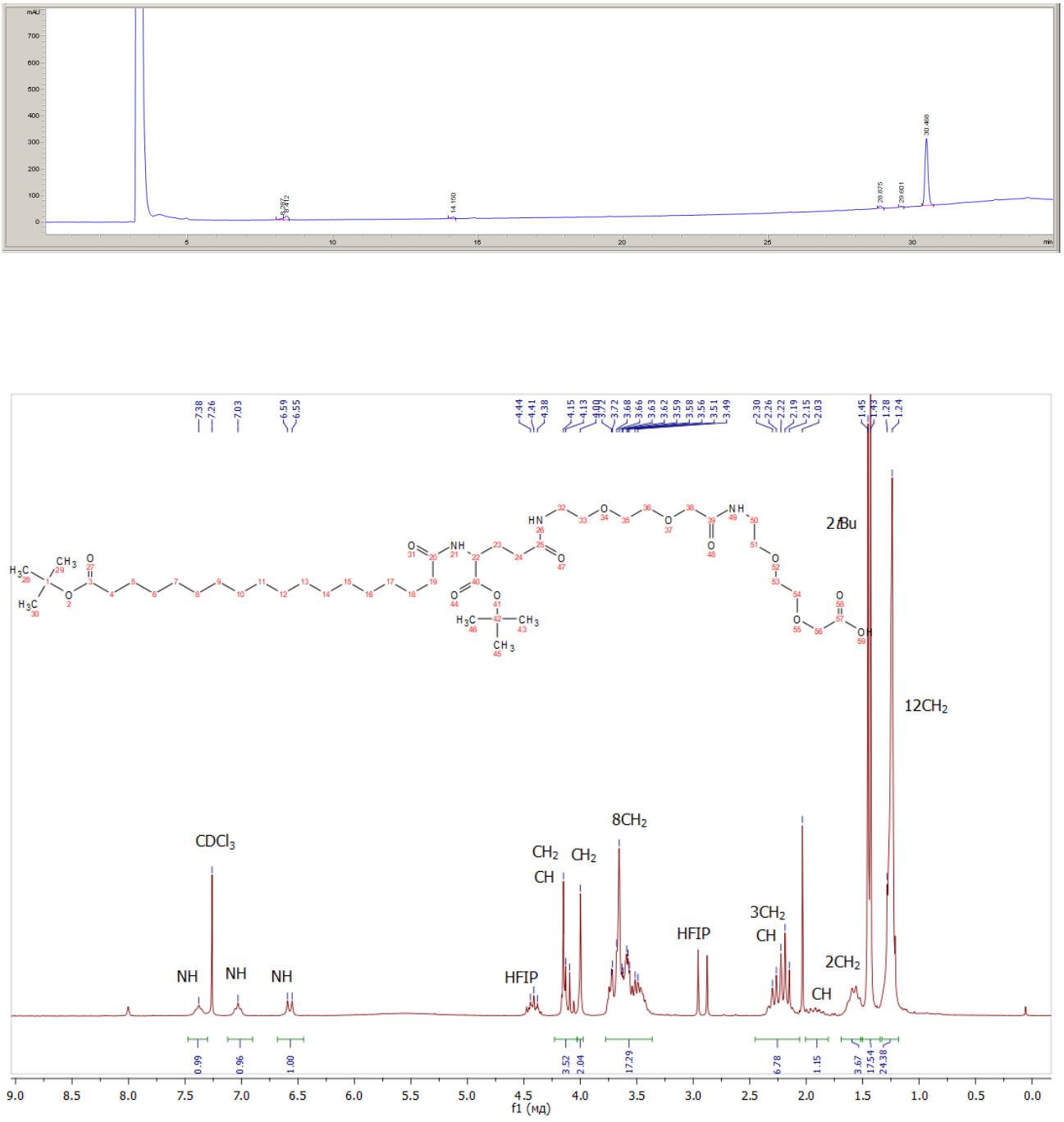

Figure S8. HPLC profile (top) and ^{1}H NMR spectrum (bottom) of *t*BuOCO-$(CH_2)_{16}$-CO-Glu(AEEA-AEEA)-O*t*Bu (Analytical method 1, see Experimental part).

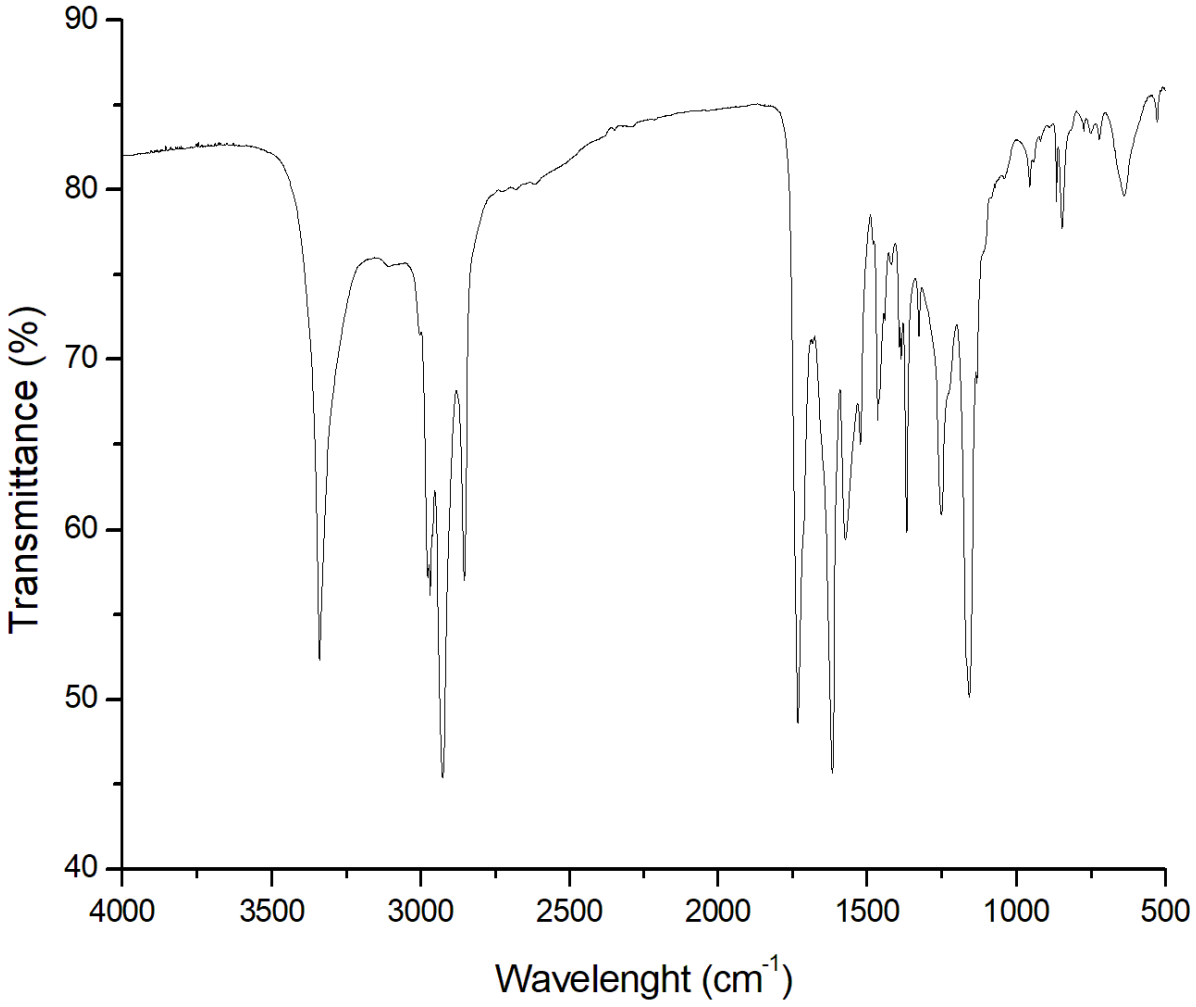

Figure S9. FT-IR spectrum of *t*BuOCO-$(CH_2)_{16}$-CO-Glu(AEEA-AEEA)-O*t*Bu (KBr).

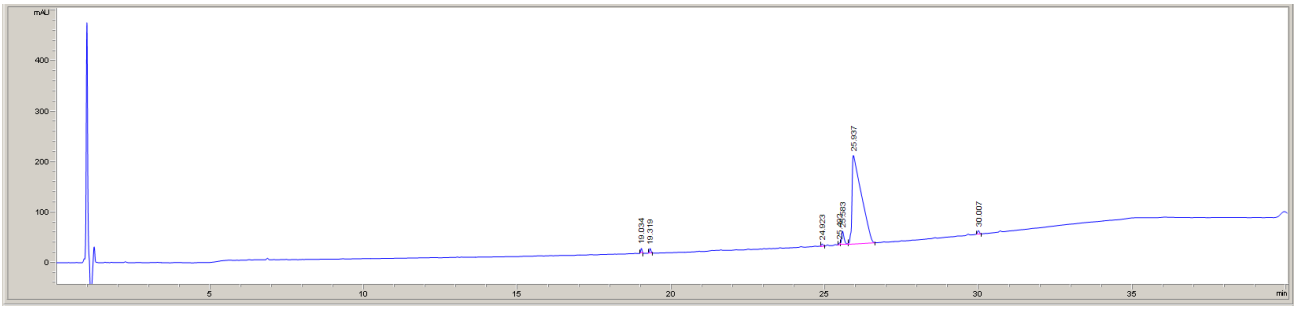

Figure S10. HPLC profile H-Lys(*t*BuOCO-$(CH_2)_{16}$-CO-Glu(AEEA-AEEA)-O*t*Bu)-OH (Analytical method 1, see Experimental part).

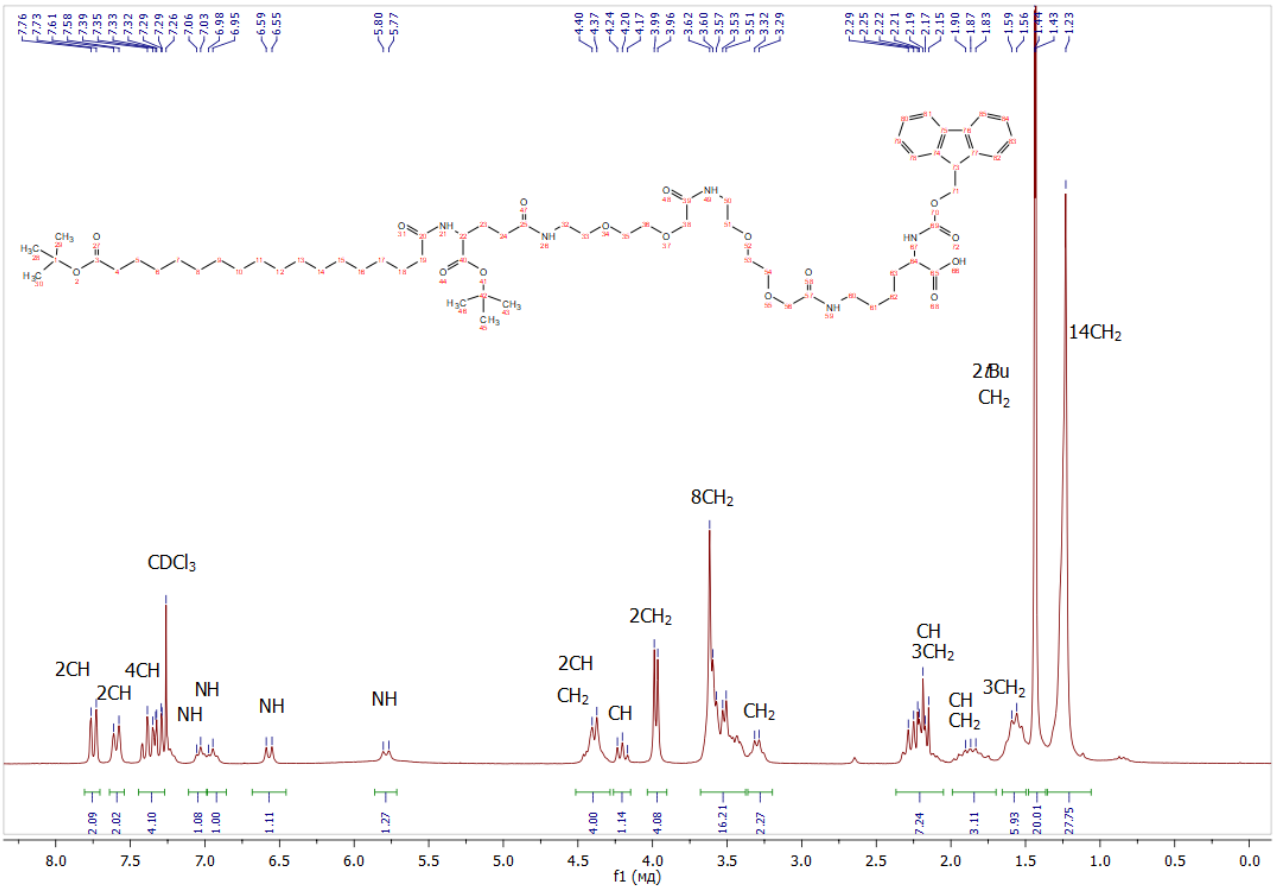

Figure S11. ^{1}H NMR spectrum of Fmoc-Lys(*t*BuOCO-$(CH_2)_{16}$-CO-Glu(AEEA-AEEA)-O*t*Bu)-OH.

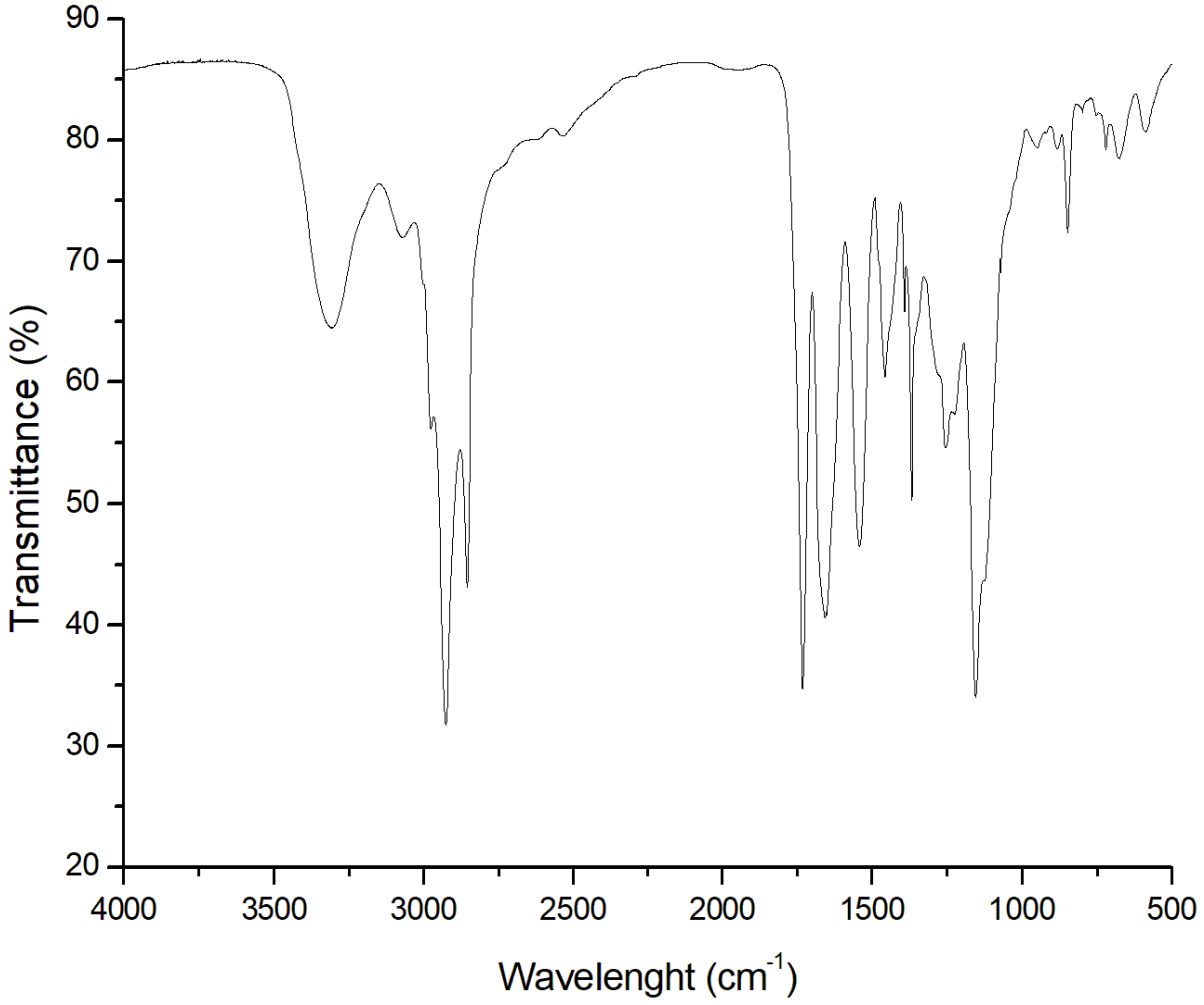

Figure S12. FT-IR spectrum of Fmoc-Lys(*t*BuOCO-$(CH_2)_{16}$-CO-Glu(AEEA-AEEA)-O*t*Bu)-OH (KBr).

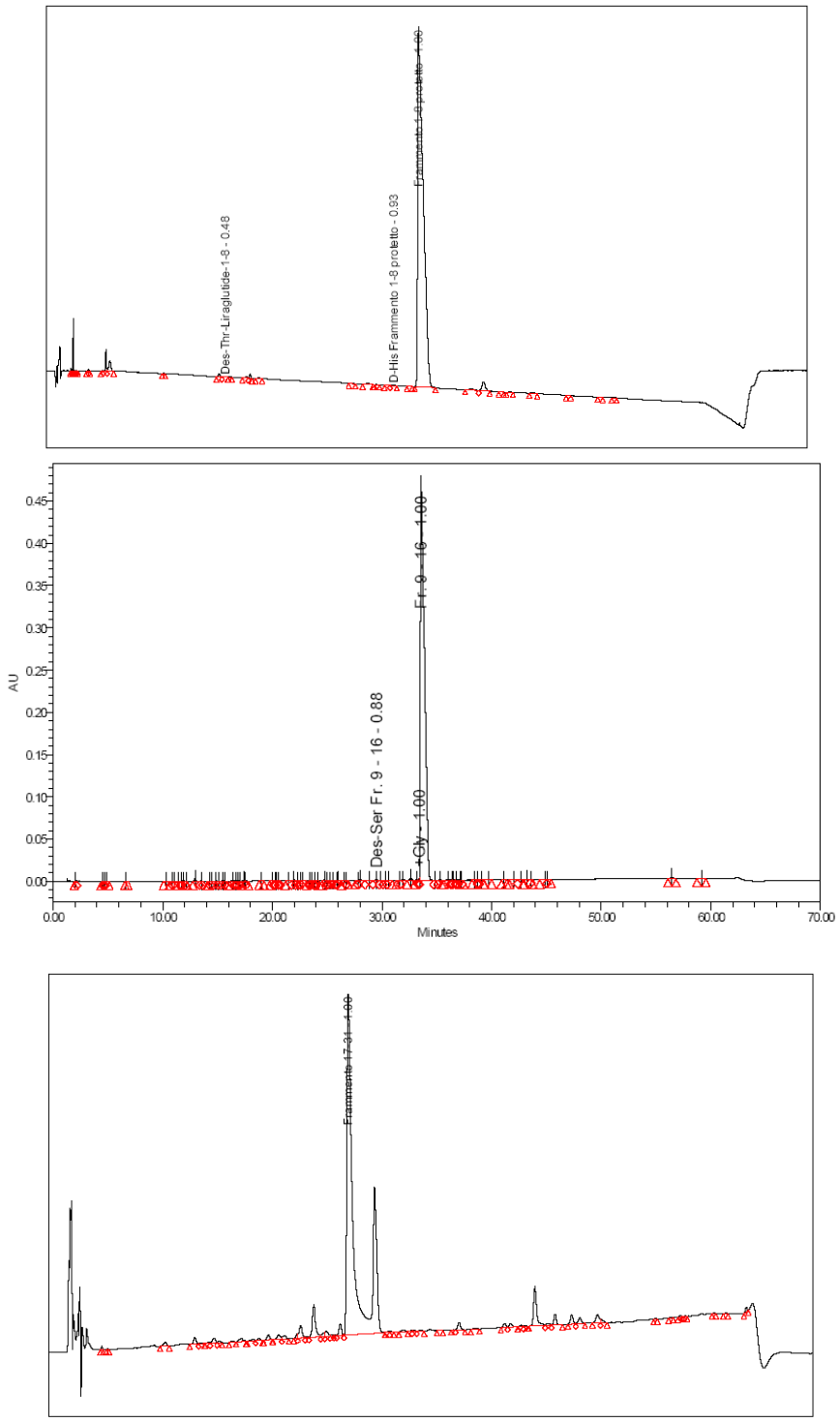

Figure S13. HPLC profiles of the protected fragments 1-8 (top), 9-16 (middle) and 17-31 (bottom) of Liraglutide (Analytical method 2 for 1-8, 3 for 9-16 and 4 for 17-31, see Experimental part).

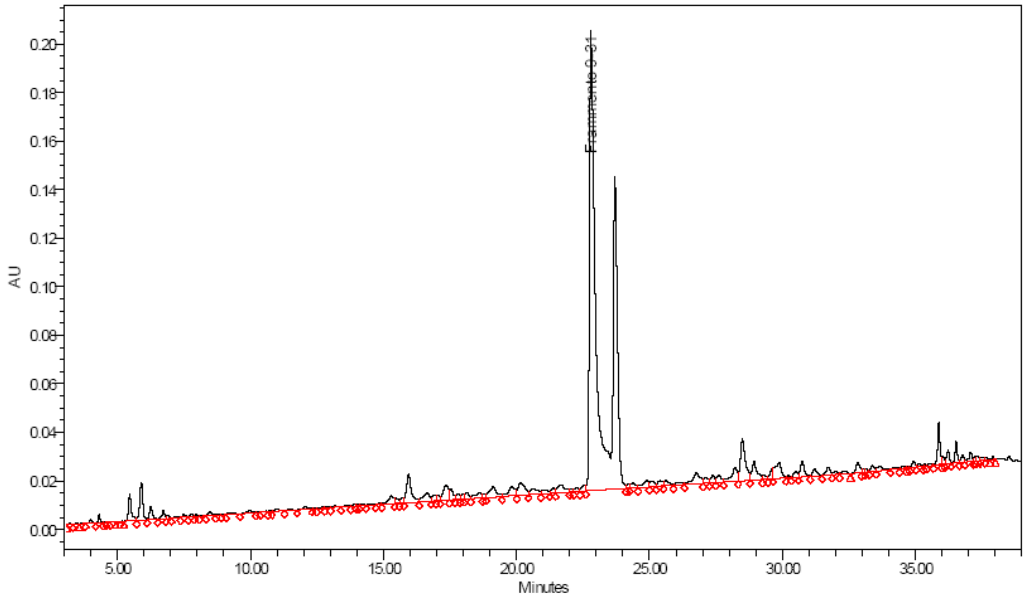

Figure S14. HPLC profile of the fragment 9-31 of Liraglutide (Analytical method 4, see Experimental part).

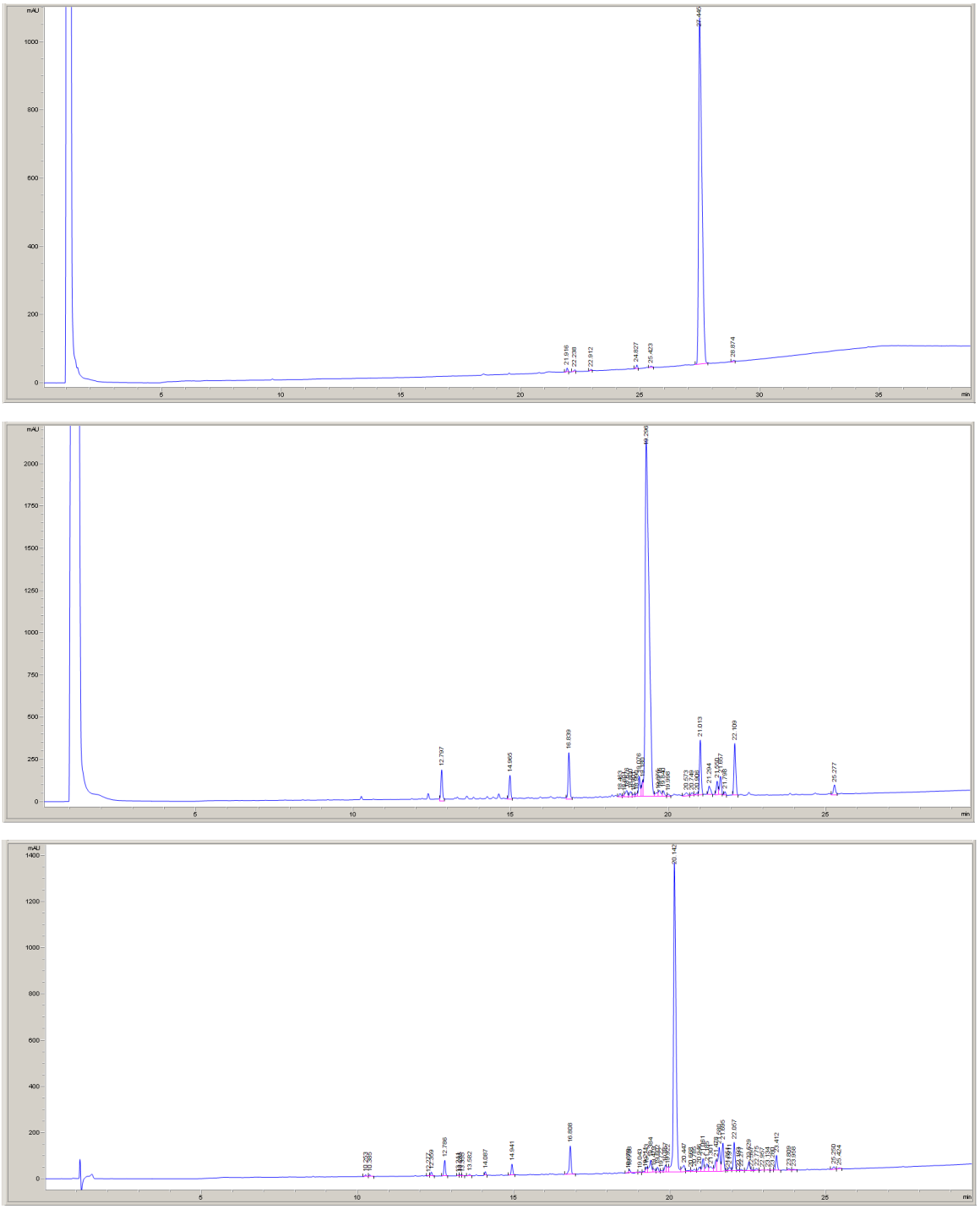

Figure S15. HPLC profiles of the protected fragment 1-8 (top) and deprotected fragments 17-31 (middle) and 9-31 (bottom) of Semaglutide (Analytical method 1, see Experimental part).

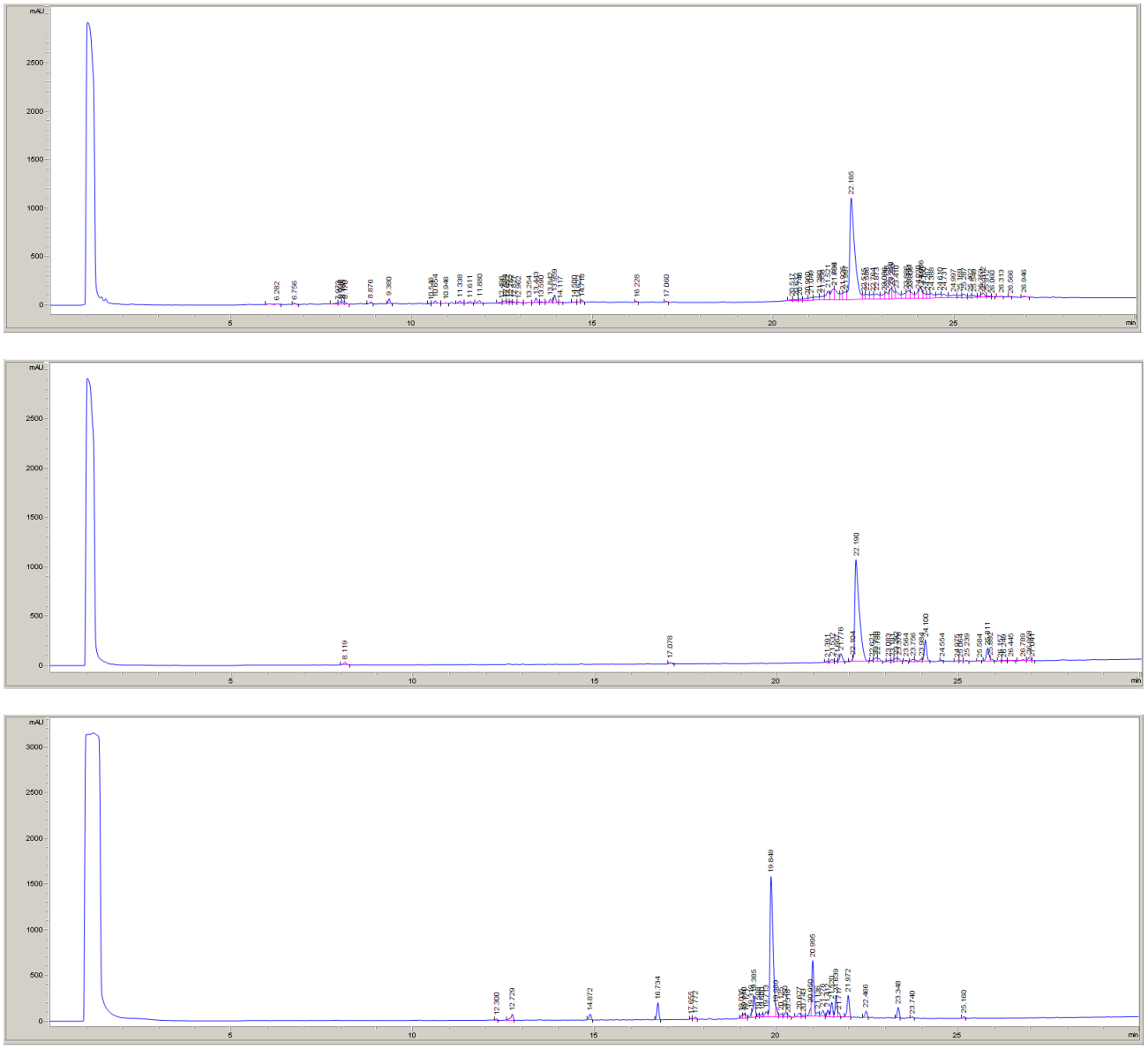

Figure S16. HPLC profiles of crude Liraglutide prepared by step-by-step SPPS (top) and crude Liraglutide and Semaglutide prepared by convergent approach (middle and bottom, respectively) (Analytical method 1, see Experimental part).

Table S1. Impurities observed in crude Liraglutide (step-by-step approach)

Entry	Retention time (min)	Area (%)	Entry	Retention time (min)	Area (%)
1	6.28	0.43	50	23.14	1.63
2	6.76	0.21	51	23.25	1.86
3	7.97	0.34	52	23.29	1.67
4	8.04	0.44	53	23.41	1.87
5	8.11	0.29	54	23.69	1.81
6	8.17	0.28	55	23.75	1.96
7	8.88	0.38	56	23.81	1.25
8	9.38	0.65	57	24.02	1.32
9	10.55	0.08	58	24.09	2.65
10	10.65	0.74	59	24.16	1.05
11	10.95	0.26	60	24.27	0.98
12	11.34	0.61	61	24.39	1.40
13	11.61	0.54	62	24.61	1.41
14	11.88	0.62	63	24.73	1.39
15	12.50	0.34	64	25.00	1.44
16	12.58	0.52	65	25.17	0.73
17	12.65	0.31	66	25.29	1.02
18	12.75	0.29	67	25.46	0.46
19	12.83	0.28	68	25.55	0.74
20	12.96	0.24	69	25.75	0.45
21	13.25	0.26	70	25.81	1.07
22	13.44	0.88	71	25.91	0.38
23	13.59	0.27	72	26.06	0.17
24	13.84	0.71	73	26.31	0.25
25	13.96	1.09	74	26.57	0.17
26	14.12	0.10	75	26.95	0.31
27	14.50	0.14			
28	14.62	0.10			
29	14.72	0.35			
30	16.23	0.17			
31	17.06	0.15			
32	20.52	0.30			
33	20.63	0.39			
34	20.75	0.45			
35	20.96	0.71			
36	21.05	0.81			
37	21.28	1.37			
38	21.36	1.07			
39	21.52	2.26			
40	21.69	2.36			
41	21.70	2.94			
42	21.93	1.26			
43	22.00	1.86			
44	**22.17**	**35.97**			
45	22.52	0.86			
46	22.59	1.23			
47	22.76	1.40			
48	22.87	1.94			
49	23.09	1.32			

Table S2. Impurities observed in crude Liraglutide (fragment approach)

Entry	Retention time (min)	Area (%)
1	8.12	1.22
2	17.08	0.40
3	21.39	0.61
4	21.53	1.30
5	21.67	0.57
6	21.78	3.44
7	22.10	0.67
8	**22.19**	**64.10**
9	22.62	0.36
10	22.73	1.46
11	22.78	1.03
12	23.08	0.97
13	23.19	0.49
14	23.28	1.40
15	23.38	1.09
16	23.56	0.61
17	23.76	1.01
18	23.98	1.72
19	24.10	7.53
20	24.55	0.31
21	24.98	0.20
22	25.06	0.29
23	25.24	0.36
24	25.58	0.23
25	25.81	5.11
26	25.89	0.73
27	26.16	0.08
28	26.25	0.19
29	26.45	0.34
30	26.79	0.78
31	26.96	1.30
32	27.04	0.09

Table S3. Impurities observed in crude Semaglutide (fragment approach)

Entry	Retention time (min)	Area (%)
1	12.30	0.37
2	12.73	1.93
3	14.87	1.25
4	16.73	3.34
5	17.66	0.30
6	17.77	0.63
7	19.04	0.55
8	19.11	0.96
9	19.17	0.37
10	19.32	1.12
11	19.39	4.43
12	19.51	0.58
13	19.60	0.80
14	19.71	1.59
15	**19.85**	**41.99**
16	19.99	1.33
17	20.13	1.00
18	20.25	1.29
19	20.32	0.35
20	20.63	1.14
21	20.74	0.41
22	20.95	1.83
23	21.00	11.09
24	21.14	1.19
25	21.28	1.53
26	21.41	1.40
27	21.52	3.05
28	21.64	4.50
29	21.72	0.57
30	21.97	4.81
31	22.47	1.40
32	23.35	2.13
33	23.74	0.26
34	25.16	0.50